High performance Pd promoted Sm$_{0.5}$Sr$_{0.5}$CoO$_3$–La$_{0.8}$Sr$_{0.2}$Ga$_{0.8}$Mg$_{0.15}$Co$_{0.05}$O$_{3-\delta}$ composite cathodes for intermediate temperature solid oxide fuel cells

Shizhong Wang [*], Hao Zhong

Department of Chemistry, Xiamen University, Xiamen 361005 Fujian, PR China

Abstract

Pd promoted Sm$_{0.5}$Sr$_{0.5}$CoO$_3$ (SSC)–La$_{0.8}$Sr$_{0.2}$Ga$_{0.8}$Mg$_{0.15}$Co$_{0.05}$O$_{3-\delta}$ (LSGMC5) composite cathodes for intermediate temperature solid oxide fuel cells (ITSOFC) were prepared using the wet impregnation method. XRD analyses demonstrated that the Pd in the electrode was in the form of PdO. The activity for oxygen reduction of the electrode increased with the increase in the concentration of Pd in the electrode and with the decrease in the electrode sintering temperature. The electrode containing 2.4 wt% Pd sintered at 1123 K showed an electrode resistance about 0.12 Ω cm^2 at near equilibrium conditions in oxygen at 873 K, which was only about one fourth of the electrode resistance without Pd addition. The addition of Pd species in the electrode showed no obvious effect on the mechanism of the oxygen reduction reaction.
© 2007 Published by Elsevier B.V.

Keywords: Solid oxide fuel cell; Cathode; SSC; Pd; Oxygen reduction

1. Introduction

The intermediate temperature solid oxide fuel cell (ITSOFC) is a leading technology for generating electricity by an efficient and environmentally friendly process. However, the reduction in operating temperature leads to a significant decrease in electrode activity. As a result, the conventional SOFC cathode, strontium doped lanthanum manganite (LSM), is not suitable for ITSOFC due to its low activity below 1073 K. There are growing interests in developing effective cathodes for the ITSOFC [1–4].

It is evident that the performance of the cathode depends strongly on the oxygen ion conductivity of the electrode. Strontium doped samarium cobaltite with a composition of Sm$_{0.5}$Sr$_{0.5}$CoO$_3$ (SSC) is one of the promising cathodes for oxygen reduction [5–10]. The stability and activity of the SSC cathode were enhanced by adding a suitable amount of La$_{0.8}$Sr$_{0.2}$Ga$_{0.8}$Mg$_{0.15}$Co$_{0.05}$O$_{3-\delta}$ (LSGMC5) into the electrode [10]. This kind of SSC–LSGMC5 composite electrode could be good candidate for the cathode of the ITSOFC based on

lanthanum gallate electrolytes, because the LSGMC5 in the electrode could be effective on improving the compatibility between the electrode and electrolyte.

The performance of a SSC–LSGMC5 composite electrode could be further improved by introducing an LSGMC5 interlayer between the SSC–LSGMC5 electrode and LSGMC5 electrolyte [11,12]. The interlayer causes the electrolyte surface to be rough, resulting in an increased three-phase boundary length and electrode/electrolyte two-phase interfacial area, i.e., an increased active reaction zone. The interlayer could also improve the bonding strength between the electrode and electrolyte. This method works well in the case that the surface of the electrolyte is smooth.

The addition of Pd or other noble metal in the electrode is another conventional method for improving the performance of SOFC cathode. Lanthanum manganite electrode supported on YSZ electrolyte has shown an improved activity after the addition of Pd supported on activated carbon [13]. The addition of Pd was also effective on improving the performance of La$_{0.6}$Sr$_{0.4}$Co$_{0.2}$Fe$_{0.8}$O$_3$ supported on doped ceria [14]. The optimum Pd loading resulted in three to four times lower cathodic impedance in the temperature range of 673–1023 K due to the electro-catalytic activity of Pd species.

---
[*] Corresponding author. Tel.: +86 592 2184968; fax: +86 592 2184968.
 E-mail address: shizwang@sohu.com (S. Wang).

So far, few reports are available on the effect of Pd species on the performance of SSC–lanthanum gallate composite electrodes supported on lanthanum gallate electrolyte. The compatibility between Pd and SSC–lanthanum gallate composite electrode is still a question.

In this study, various Pd promoted SSC–LSGMC5 composite electrodes were prepared. The synthesizing parameters were optimized, and the kinetic characteristics of typical electrodes were studied in detail using multiple techniques.

2. Experimental

$La_{0.8}Sr_{0.2}Ga_{0.8}Mg_{0.15}Co_{0.05}O_{3-\delta}$ (LSGMC5) electrolyte was prepared using the conventional solid-state reaction [10–12]. The electrolyte in the shape of disk was sintered at 1748 K for 6 h in air, and then polished to a thickness of about 0.3 mm. The diameter of the sintered pellet was about 15 mm.

Pd modified $Sm_{0.5}Sr_{0.5}CoO_3$ (SSC)–LSGMC5 composite cathodes were prepared using the wet impregnation method. First, SSC–LSGMC5 composite powders were obtained by mixing and grinding the SSC powders sintered at 1323 K for 12 h and LSGMC5 powders sintered at 1473 K for 6 h. The SSC and LSGMC5 powders were synthesized using the conventional solid-state reaction as reported previously [10], and the weight percentage of SSC in the electrode was about 85 wt%. Then, a stoichiometric amount of SSC–LSGMC5 powder was added into a beaker containing a suitable amount of 0.05 M $PdCl_2$ solution. After boiling and drying under continuous stirring, the mixture was sintered at 1073 K for 1 h. Four kinds of electrodes were prepared, in which the weight percentage of Pd element in the electrode was 0, 0.6, 1.2 and 2.4 wt%, respectively.

The phase compositions of SSC–LSGMC5 composite powders and LSGMC5 powders containing 2.4 wt% Pd were examined using X-ray diffractometer (XRD, Panalytical X'pert). The samples were sintered at 1123 and 1373 K, respectively, to examine the chemical compatibility between Pd and other materials, i.e., SSC and LSGMC5. The LSGMC5 powders examined were the same as those in the SSC–LSGMC5 composite cathode.

Electrochemical properties of the electrodes were characterized using a three-electrode system as reported previously [10–12]. A 2–5 μm LSGMC5 interlayer was deposited on the surface of the electrolyte and sintered at 1673 K before the printing of the electrode. LSGMC5 powder used for preparing the interlayer was synthesized using the citrate method [12]. Symmetrical Pd promoted SSC–LSGMC5 composite electrodes were then screen-printed on the LSGMC5 interlayer and sintered at 1123–1223 K for 2 h. The areas of the electrodes were about 0.2 cm^2, which were the same as those of the LSGMC5 interlayer. The thickness of the electrode was typically about 20 μm. A Pt reference electrode was prepared on the same side of the working electrode and sintered at 1073 K for 2 h. The three-electrode cell was characterized in a mixture of N_2 (99.99%) and O_2 (99.99%) with a total flow rate of 100 ml min^{-1}. The oxygen partial pressure of the mixture was in the range of 2×10^3 to 1×10^5 Pa, which was determined using a zirconia oxygen sensor.

All of the electrochemical measurements including dc polarization and ac impedance measurements were carried out with a VMP2/Z-40 (AMETEK) electrochemical testing station. The frequency range for the impedance measurements was usually 0.01 Hz–100 kHz, and the amplitude of the input sinuous signal was 10 mV. Electrochemical measurements were carried out on samples of which the impedance of the two-electrode measurement was about twice of the three-electrode measurement (within 10% error) [10,15].

The spent samples were examined using a scanning electron microscopy (Leo1530) equipped with an energy dispersive X-ray spectrometer (EDS).

3. Results and discussion

3.1. Phase composition

Shown in Fig. 1 are the XRD patterns of various SSC–LSGMC5 composite powders and LSGMC5 powders containing 2.4 wt% Pd. Phases corresponding to SSC [6] and LSGMC5 [16] can be identified in the Pd promoted SSC–LSGMC5 composite electrodes. No new phases are observed. However, phases corresponding to PdO and LSGMC5 are observed in Pd coated LSGMC5. Further, the strength of the peaks corresponding to PdO decrease with increasing sintering temperatures. There should also be a PdO phase in the Pd modified SSC–LSGMC5 composite electrode, however, it cannot be identified since the peaks corresponding to PdO are overlapped by the peaks corresponding to SSC as shown in Fig. 1. PdO should be the major phase for Pd species in air at high temperatures according to literature [13,14,17]. Fig. 1 suggests a good chemical compatibility between Pd species and SSC–LSGMC5 electrode even under high sintering temperatures.

3.2. Microstructure

Shown in Fig. 2 are the SEM images of the cross-section of SSC–LSGMC5 composite electrodes containing 0 or 2.4 wt%
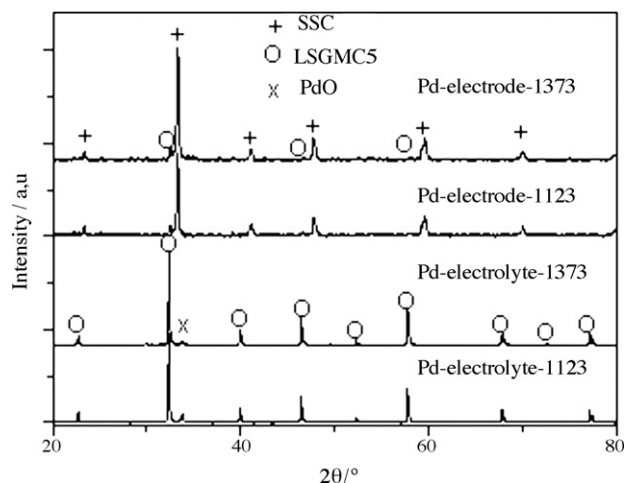
Fig. 1. XRD patterns of the SSC–LSGMC5 electrode and LSGMC5 electrolyte containing 2.4 wt% Pd sintered at 1373 and 1123 K, respectively.
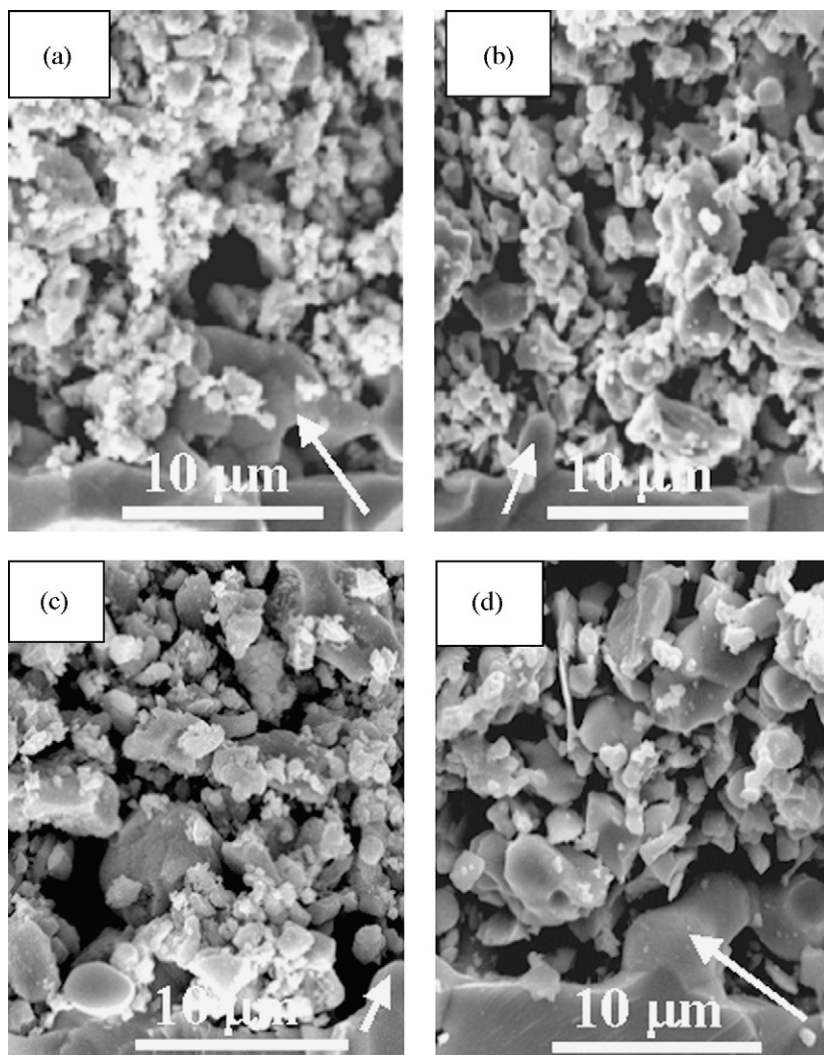
Fig. 2. SEM images of the cross section of various SSC–LSGMC5 electrodes: (a) containing 2.4 wt% Pd, sintered at 1123 K; (b) no Pd, sintered at 1123 K; (c) containing 2.4 wt% Pd, sintered at 1223 K; (d) no Pd, sintered at 1223 K. The arrow in the image indicates the interlayer between the electrode and electrolyte.

Pd sintered at 1123 and 1223 K, respectively. The electrodes sintered at 1123 K exhibit smaller electrode particles and higher porosities compared with those sintered at 1223 K [12]. Moreover, the surface of the electrode particles without Pd addition is glossy as seen in Fig. 2(b and d). However, the appearance of the surface of the electrode particles changes dramatically after the addition of Pd, which suggests that the surface of the electrode is covered with a very thin layer of PdO particles. Some relatively big PdO particles could also exist on the surface of the electrode, because there are more small particles in the electrode containing Pd compared with that without Pd addition. However, all the appearances of the small particles are quite similar, therefore, it is difficult to identify the PdO particles. The number of small particles decreases with increasing sintering temperatures, suggesting a strong dependency of PdO distribution on the sintering temperature.

The results of the EDS analyses show that the ratio of Pd to Sm decreases from 0.15 for the electrode sintered at 1123 K to 0.08 for the electrode sintered at 1223 K, which agrees with the results in Fig. 2. The results in the literature also showed that the

distribution of supported PdO species depended strongly on the sintering temperature and aging time of the sample [18]. The strong sintering temperature dependency of PdO distribution could also be the main reason leading to the decrease in the strength of XRD peaks corresponding to PdO at high sintering temperatures.

3.3. Electrochemical characterization

3.3.1. Effect of the concentration of Pd in the electrode

Shown in Fig. 3 are the impedance spectra at open circuit voltage (OCV) in oxygen at 873 K of SSC–LSGMC5 cathodes containing various amount of Pd sintered at 1123 K. One major arc at intermediate frequency can be observed in the spectra besides a small arc at high frequency. The arc at high frequency is usually less then 5% of the overall spectrum at OCV. This high frequency arc could correspond to the transfer of oxygen ions across the electrode/electrolyte interface [10–12]. The size of the spectrum decreases with increasing amount of Pd in the electrode, which is due dominantly to the decease in the size
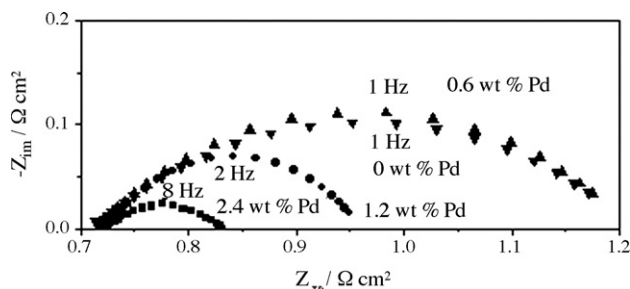
Fig. 3. Impedance spectra at OCV in oxygen at 873 K of SSC–LSGMC5 electrodes containing various concentration of Pd.

of the arc at intermediate frequency. The electrode containing 2.4 wt% Pd shows an electrode resistance about $0.12\,\Omega\,cm^2$ at OCV in oxygen at 873 K, which is only about one fourth of the electrode without Pd addition [12]. The ohmic resistance of the electrode, which can be read from the high frequency intercept of the spectrum, shows no obvious dependency on the amount of Pd in the electrode. It is clear that the Pd added in the composite electrode is effective on improving the activity for oxygen reduction reaction.

Shown in Fig. 4 are the temperature dependencies of T/R_p of various electrodes. R_p is the overall polarization resistance of the electrode measured using impedance spectrometry. The activity of the electrode increases with increasing concentration of Pd in the electrode at all the temperatures studied. The relative decrease in electrode polarization resistance increases with decreasing reaction temperatures as estimated from Fig. 4. For an example, the electrode resistance decreases from 0.46 to $0.12\,\Omega\,cm^2$ at 873 K and from 0.020 to $0.0082\,\Omega\,cm^2$ at 1073 K after the addition of 2.4 wt% Pd. This result suggests that the addition of Pd is more effective on improving the electrode performance at low temperatures as reported in references [13,14].

The activation energy of T/R_p of the electrode containing high concentration of Pd is slightly lower than that of the electrode without Pd addition. For an example, the activation energy of T/R_p of the electrode containing 2.4 wt% Pd is about $122\,kJ\,mol^{-1}$, which is about 10% lower than that of the elec-
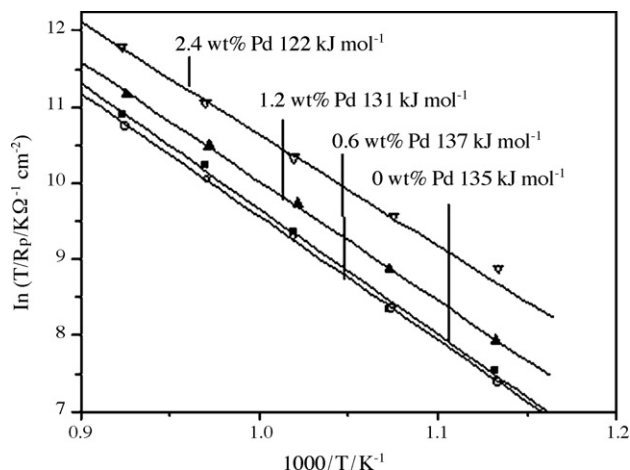
Fig. 4. T/R_p in oxygen of SSC–LSGMC5 electrodes containing various concentration of Pd as a function of temperature.
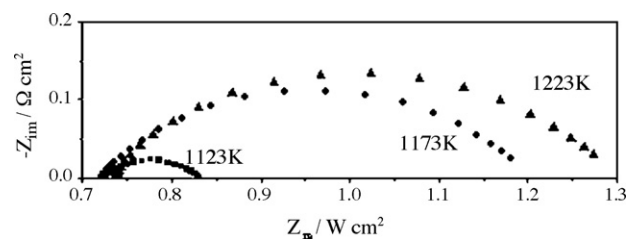
Fig. 5. Impedance spectra at OCV in oxygen at 873 K of SSC–LSGMC5 containing 2.4 wt% Pd sintered at various temperatures.

trode without Pd addition. The activation energy calculated using the overall polarization resistance is very close to that calculated using the impedance of the arc at intermediate frequency (within 1–2% relative error, which will be shown later). This is because that the arc at intermediate frequency is the dominant part of the overall spectrum.

3.3.2. Effect of the sintering temperature

Shown in Fig. 5 are the impedance spectra at 873 K in oxygen of SSC–LSGMC5 electrodes containing 2.4 wt% Pd sintered at various temperatures. It is clear that the impedance of the electrode sintered at 1123 K is much smaller than that sintered at 1173 and 1223 K. With further decrease in the sintering temperature of the electrode, the bonding between the electrode and electrolyte is rather weak, and no stable electrochemical measurements can be carried out. Shown in Table 1 are the electrode polarization resistances at 973 K in oxygen at OCV of SSC–LSGMC5 added with 2.4 wt% Pd sintered at various temperatures. The electrode polarization resistances of SSC–LSGMC5 without Pd addition sintered at various temperatures are shown in the same table [12]. As it can be seen from Table 1, both the electrode polarization resistances of SSC–LSGMC5 and SSC–LSGMC5 containing 2.4 wt% Pd increase with electrode sintering temperatures. However, the electrode polarization resistances of SSC–LSGMC5 are always higher than those of corresponding Pd promoted electrodes. Furthermore, the ratio of the electrode polarization resistance of SSC–LSGMC5 containing Pd to that without Pd addition increases dramatically with increasing sintering temperatures. It is clear that low sintering temperature is preferred for the preparation of Pd promoted SSC–LSGMC5 electrode.

Shown in Fig. 6 are the temperature dependencies of T/R_p for various electrodes. The activity of the electrode decreases with the increase in the sintering temperature of the electrode at various operating temperatures. The activation energies of the electrodes sintered at high temperatures are higher than that sintered at 1123 K.

Table 1
Electrode polarization resistances ($\Omega\,cm^2$) at 973 K under OCV in oxygen of SSC–LSGMC5 and SSC–LSGMC5 containing 2.4 wt% Pd sintered at various temperatures

	SSC–LSGMC5 (Ref [12])	SSC–LSGMC5-2.4 wt% Pd
1123 K	0.08	0.03
1173 K	0.14	0.09
1223 K	0.18	0.11
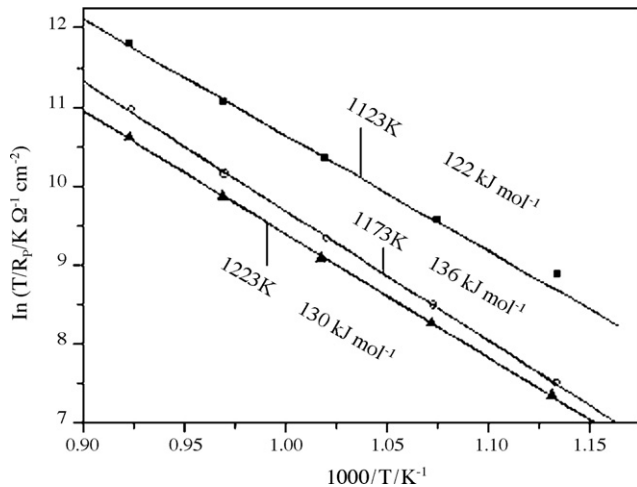
Fig. 6. T/R_p in oxygen of SSC–LSGMC5 containing 2.4 wt% Pd sintered at various temperatures as a function of temperature.

3.3.3. Kinetics of oxygen reduction over SSC–LSGMC5 containing 2.4 wt% Pd

Shown in Fig. 7(a and b) are the impedance spectra of SSC–LSGMC5 containing 2.4 wt% Pd at OCV under various oxygen partial pressures at 873 and 973 K, respectively.

As it can be seen from Fig. 7(a), one major arc at intermediate frequency appears in the impedance spectra at 873 K besides a very small arc at high frequency. The size of the arc at intermediate frequency increases with decreasing oxygen partial pressures. One more arc at low frequency appears in the spectra at 973 K under low oxygen partial pressures as shown in Fig. 7(b), the size of which depends strongly on oxygen partial pressure.

The impedance spectra in Fig. 7 can be best fitted using the equivalent circuit $LR_{el}(C(R(Q_1R_1)(Q_2R_2)))$ under low oxygen partial pressures and high temperatures, and using $LR_{el}(C(R(Q_1R_1)))$ at low temperatures and high oxygen partial pressures [12]. Where, L is the inductance, R_{el} the ohmic resistance of the cell, C the interfacial capacity. Q_1 and Q_2 are constant phase elements. R, R_1 and R_2 are the resistances corresponding to the arc at high frequency, intermediate frequency and low frequency, respectively. The R in this equivalent circuit is usually far less than 5% of the overall spectra especially at low temperatures, which corresponds to a very small arc at high frequency in the spectra. The appearance of a small arc at high frequency in the impedance spectra is often reported in the literature [3,10–12]. This arc could be related to the transfer of oxygen ions across the electrode/electrolyte interface since it has no dependency on oxygen partial pressure. Only arcs corresponding to Q_1R_1 and Q_2R_2 are analyzed in this study since they are the major parts of the spectra. The two arcs are defined as arc1 and arc2 [12], which appear at the intermediate frequency and low frequency, respectively.
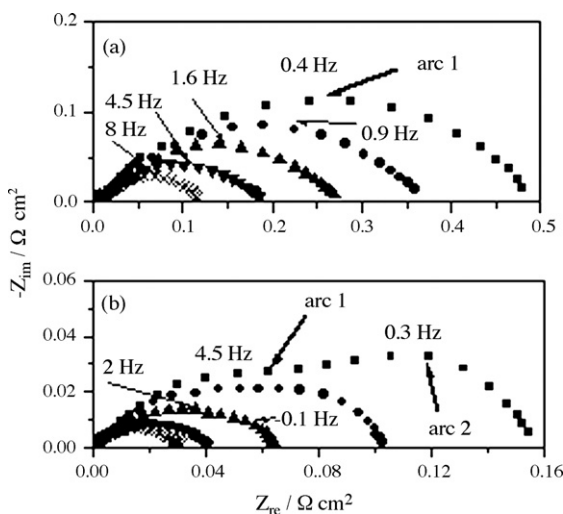
T/R_1 and T/R_2 of SSC–LSGMC5 containing 2.4 wt% Pd as a function of oxygen partial pressure at various temperatures are shown in Fig. 8 [10–12]. It is clear that T/R_1 has a pO_2 dependency about 1/2 within the temperature range of 1073–873 K, and decreases to 0.34 at 773 K. The process with a pO_2 dependency of 1/2 could be related to the surface diffusion of oxygen atom [10,19] or the dissociative adsorption of oxygen [3,7]. The process with a pO_2 dependency of 1/4 could be related to the charge transfer process [3,7,10]. The results in Fig. 8 suggest that the rate-determining step for oxygen reduction at OCV over the SSC–LSGMC5 electrode containing 2.4 wt% Pd could have a strong dependency on reaction temperatures. The oxygen reduction reaction at OCV could be controlled by the surface diffusion of oxygen atom or the dissociative adsorption of oxygen as long as the reaction temperature is higher than 873 K. The rds could change to a charge transfer process at a temperature lower than 773 K. These processes could not be separated using impedance spectrometry in this study, which is due probably to the very close time constants for these processes [10]. The change in the coverage of adsorbed oxygen species could also affect the oxygen partial pressure dependency of polarization resistance [4,20]. However, it is difficult to judge the exact reason simply based on the apparent kinetic study under OCV alone.

Fig. 7. Impedance spectra of SSC–LSGMC5 containing 2.4 wt% Pd under various oxygen partial pressures at: (a) 873 and (b) 973 K, respectively: (■) 5×10^3 Pa; (●) 1×10^4 Pa; (▲) 2×10^4 Pa; (▼) 5×10^4 Pa; (×) 1×10^5 Pa.
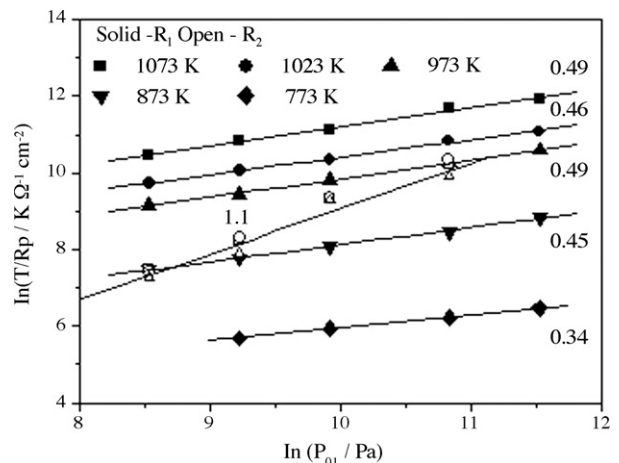
Fig. 8. T/R_1 and T/R_2 of SSC–LSGMC5 containing 2.4 wt% Pd as a function of oxygen partial pressure at various temperatures. The figures near the lines are the slope of each line.
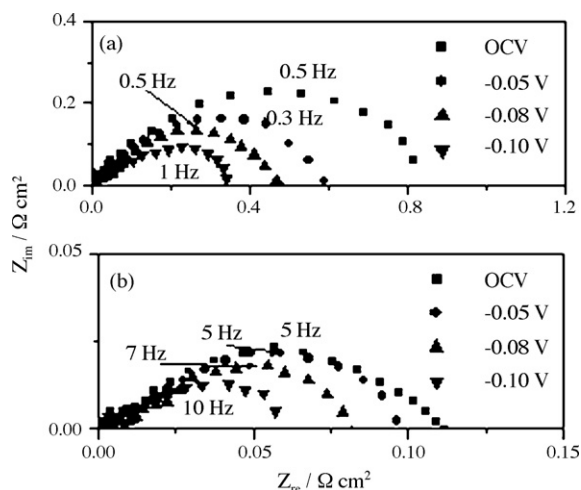
Fig. 9. Impedance spectra of SSC–LSGMC5 containing 2.4 wt% Pd in oxygen under polarization at: (a) 873 and (b) 973 K, respectively.

The activation energy of T/R_1 is about $122 \pm 3\,kJ\,mol^{-1}$ within the temperature range of 1073–873 K and the oxygen partial pressure range of 1×10^5 to 5×10^3 Pa, which is close to the results shown in Fig. 4.

The pO_2 dependency of T/R_2 is about 1 as it can be seen from Fig. 8. Further, T/R_2 is almost independent of temperature, suggesting a very low activation energy. Therefore, arc2 could correspond to the gas diffusion of oxygen [11,12,21,22]. Gas diffusion process only appears at a temperature about or higher than 973 K as it can be seen from Figs. 7 and 8.

Impedance spectra of SSC–LSGMC5 containing 2.4 wt% Pd under dc polarization in oxygen at 773 and 873 K are shown in Fig. 9(a and b), respectively. It is clear that the size of the spectrum decreases with increasing polarization overpotential at both 773 and 873 K. Moreover, the size of the arc at high frequency is almost independent of polarization overpotential, which confirms that the arc at high frequency could correspond to the transfer of oxygen ions. The arc at intermediate frequency, which decreases with increasing overpotential, could correspond to a charge transfer related process.

Impedance spectra of SSC–LSGMC5 containing 2.4 wt% Pd under dc polarization in 5×10^4, 2×10^4 and 1×10^4 Pa oxygen partial pressures at 773 and 873 K are also recorded. All the spectra decease with increasing cathodic overpotential, suggesting that no gas diffusion takes place under these experimental conditions.

Polarization curves under various oxygen partial pressures at 873 K of SSC–LSGMC5 containing 2.4 wt% Pd are shown in Fig. 10, which can be well simulated with the Butler-Volmer equation (Eq. (1)). The potential in Fig. 10 is referred to 1 atm oxygen.

$$i = i_0 \left[\exp\left(\frac{\alpha_a F \eta}{RT} \right) - \exp\left(\frac{-\alpha_c F \eta}{RT} \right) \right] \qquad (1)$$

Here, i_0 is the exchange current density, F the Faraday's constant, R the universal gas constant, T the absolute temperature and α_a and α_c are the anodic and cathodic charge transfer coefficients, respectively.

Table 2
Exchange current densities and Tafel coefficients (α_a, α_c) of SSC–LSGMC5 containing 0 and 2.4 wt% Pd under various oxygen partial pressures at 873 K

	0% Pd			2.4 wt% Pd		
	i_0	α_a	α_c	i_0	α_a	α_c
100 kPa	0.073	0.9	1.0	0.22	1.1	0.9
50 kPa	0.059	1.0	0.9	0.17	1.1	1.1
20 kPa	0.048	1.0	0.9	0.15	0.9	0.9
10 kPa	0.041	1.0	1.0	0.12	1.1	0.8

The exchange current densities and cathodic and anodic charge transfer coefficients extracted from Fig. 10 using Eq. (1) are shown in Table 2. The kinetic parameters of SSC–LSGMC5 without Pd addition are shown in the same table. The cathodic and anodic charge transfer coefficients are close to 1 even under 1×10^4 Pa oxygen partial pressure for both of the two electrodes. However, the exchange current density of SSC–LSGMC5 electrode is much lower than that of the electrode containing 2.4 wt% Pd.

The anodic current density under high overpotential shows no dependency on oxygen partial pressure as it can be seen from Fig. 10. However, the cathodic current density under high overpotential increases dramatically with increasing oxygen partial pressures. The pO_2 dependencies of i_0 and cathodic current density at an electrode potential of −0.15 V referred to 1 atm oxygen of SSC–LSGMC5 containing 2.4 wt% Pd are shown in Fig. 11. The cathodic current density at an electrode potential of −0.15 V under 1×10^5 and 5×10^4 Pa oxygen partial pressures are simulated using Eq. (1). It can be seen from Fig. 11 that the pO_2 dependency of i_0 is about 1/4, and the pO_2 dependency of cathodic current at an electrode potential of −0.15 V referred to 1.01×10^5 Pa oxygen is about 0.6.

The results of polarization measurements demonstrate that the rate-determining step for oxygen reduction over the SSC–LSGMC5 containing 2.4 wt% Pd is charge transfer under high overpotential [10–12,20], which is the same as that of the SSC–LSGMC5 cathode without Pd addition. Taking the results
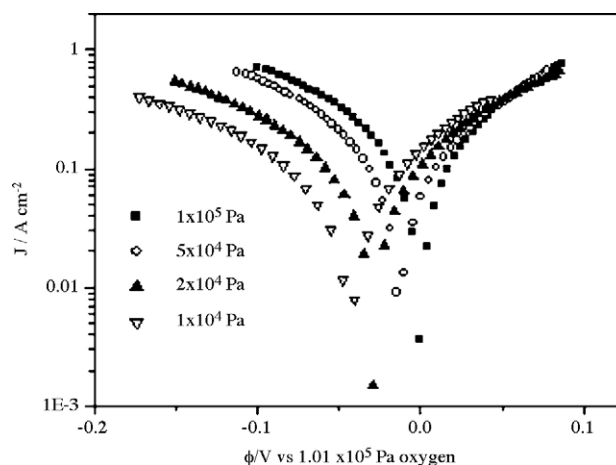
Fig. 10. Polarization curves of SSC–LSGMC5 containing 2.4 wt% Pd under various oxygen partial pressures at 873 K. The potential is referred to 1.01×10^5 Pa oxygen.
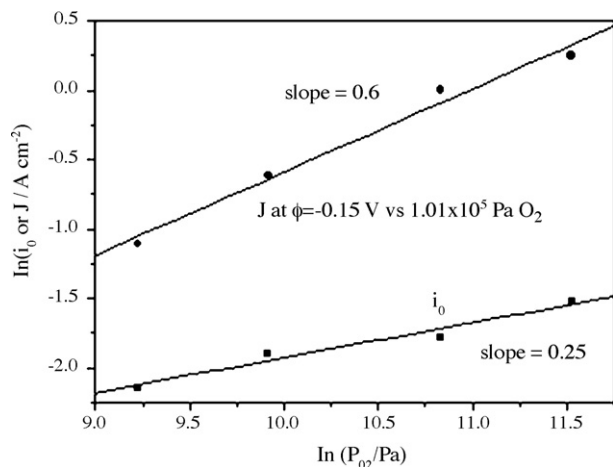
Fig. 11. Oxygen partial pressure dependencies of exchange current density and current density at -0.15 V electrode potential referred to 1.01×10^5 Pa oxygen at 873 K of SSC–LSGMC5 containing 2.4 wt% Pd sintered at 1123 K.

at OCV into consideration, it is clear that the reaction mechanism of oxygen reduction over the SSC–LSGMC5 electrode added with Pd depends strongly on the reaction temperature, oxygen partial pressure and overpotential as reported previously [10–12]. The strong dependency of reaction mechanism on operating conditions is quite reasonable, because the oxygen reduction reaction over mixed ionic–electronic conductors is typically a complex multi-pathway reaction in nature [10,23,24].

The improved performance of SSC–LSGMC5 electrode after the addition of Pd could be due to the extension of active reaction zone or the increase in reaction rate of each active reaction site. However, it is generally accepted that the extension of active reaction zone is mainly determined by the oxygen ion conductivity of the electrode [23,24]. Because Pd species in the electrode would not have significant effect on the oxygen ion conductivity of the electrode, the extension of active reaction zone could be very limited.

Effects of Pd addition on the tracer diffusion (D^*) and surface exchange (k) coefficients of oxygen over porous $La_{0.6}Sr_{0.4}Co_{0.2}Fe_{0.8}O_3$ electrodes supported on $Ce_{0.9}Gd_{0.1}O_{1.95}$ electrolyte have been reported [13]. D^* was not significantly affected but k decreased by well over an order of magnitude with Pd loadings. Therefore, it is most likely that Pd could not improve the diffusion of oxygen atoms and the surface exchange of oxygen significantly. It is expected that the improvement in electrode activity after the addition of Pd could be due to the high electrocatalytic activity of Pd species [13], because the Pd added is effective on improving the performance of the electrode under OCV as well as polarization despite of the change in reaction mechanism.

4. Conclusions

Pd, which was in the form of PdO, was effective on improving the performance of $Sm_{0.5}Sr_{0.5}CoO_3$ (SSC)–$La_{0.8}Sr_{0.2}$ $Ga_{0.8}Mg_{0.15}Co_{0.05}O_{3-\delta}$ (LSGMC5) composite cathodes. Pd showed good chemical compatibility with both SSC and LSGMC5. The activity for oxygen reduction of the electrode increased with increase in the concentration of Pd in the electrode and with the decrease in the sintering temperature of the electrode. The introduction of Pd in the electrode showed no obvious effect on the oxygen reduction mechanism. The reaction mechanism depended strongly on the operating conditions.

References

[1] E.P. Murray, M.J. Sever, S.A. Barnett, Solid State Ionics 148 (2002) 27–34.
[2] V. Dusastre, J.A. Kilner, Solid State Ionics 126 (1999) 163–174.
[3] S. Wang, Y. Jiang, Y. Zhan, J. Yan, W. Li, J. Electrochem. Soc. 145 (1998) 1932–1939.
[4] Y. Jiang, S. Wang, Y. Zhang, J. Yan, W. Li, Solid State Ionics 110 (1998) 111–119.
[5] H. Fukunaga, M. Koyama, N. Takahashi, C. Wen, K. Yamada, Solid State Ionics 132 (2000) 279–285.
[6] C. Xia, E. Rauch, F. Chen, M. Liu, Solid State Ionics 149 (2002) 11–19.
[7] M. Koyama, C. Wen, T. Masuyama, J. Otomo, H. Fukunaga, K. Yamada, K. Eguchi, H. Takahashi, J. Electrochem. Soc. 148 (2001) A795–A801.
[8] H.Y. Tu, Y. Takeda, N. Imanishi, O. Yamamoto, Solid State Ionics 100 (1997) 283–288.
[9] T. Ishihara, M. Honda, T. Shibayama, H. Minami, H. Nishiguchi, Y. Takita, J. Electrochem. Soc. 145 (1998) 3177–3183.
[10] S. Wang, T. Chen, S. Chen, J. Electrochem. Soc. 151 (2004) A1461–A1467.
[11] S. Wang, H. Zhong, Q. Dong, Electrochim. Acta 52 (2007) 1936–1941.
[12] S. Wang, H. Zhong, Y. Zou, J. Power Sources 161 (2006) 1154–1160.
[13] V.A.C. Haanappel, D. Rutenbeck, A. Mai, S. Uhlenbruck, H. Wesemeyer, B.R. Wekamp, C. Tropartz, F. Tietz, J. Power Sources 130 (2004) 119–128.
[14] M. Sahibzada, S.J. Benson, R.A. Rudkin, J.A. Kilner, Solid State Ionics 113–115 (1998) 285–290.
[15] H. Hu, M. Liu, Solid State Ionics 109 (1998) 259–272.
[16] S. Wang, Y. Zou, Electrochem. Commun. 8 (2006) 927–931.
[17] E.H. Voogt, A.J.M. Mens, O.L.J. Gijzeman, J.W. Geus, Surf. Sci. 350 (1996) 21–31.
[18] A.K. Datye, Q. Xu, K.C. Khara, J.M. McCarty, Catal. Today 111 (2006) 59–64.
[19] C. Schwandt, W. Weppner, J. Electrochem. Soc. 144 (1997) 3728–3736.
[20] F.H. Van Heuveln, H.J.M. Bouwmeester, J. Electrochem. Soc. 144 (1997) 134–140.
[21] S. Yoon, S. Nama, J. Hana, T. Lima, S. Hong, Solid State Ionics 166 (2004) 1–11.
[22] S. Primdahl, M. Mogensen, J. Electrochem. Soc. 145 (1998) 2431–2438.
[23] M. Liu, J. Electrochem. Soc. 145 (1998) 142–154.
[24] S.B. Adler, J.A. Lane, B.C.H. Steele, J. Electrochem. Soc. 143 (1996) 3554–3564.